

# INVESTIGATION OF THE PRODUCTION OF TRICLOSAN/CHITOSAN NANOCAPSULES FOR FUNCTIONAL SURFACE APPLICATIONS

DASDEMIR, MEHMET<sup>1,2</sup>; SERDAR, SERAP GAMZE<sup>2\*</sup> AND IBILI, HATICE<sup>2</sup>

<sup>1</sup> The Nonwovens Institute, North Carolina State University, Raleigh, NC 27606, USA

<sup>2</sup> Gaziantep University, Textile Engineering Department, Gaziantep, 27310, Turkey

## ABSTRACT

This study focuses on producing monodisperse nanocapsules with a triclosan/chitosan core-shell structure using the coaxial electrospray method. The coaxial electrospraying method enables the production of core/shell structured nanocapsules in a single step. The effects of flow rate, core-to-shell flow rate ratio, and needle size on the coaxial electrospray process were systematically analyzed. The resulting nanocapsule structures were characterized using scanning electron microscope (SEM), transmission electron microscope (TEM) and size measurements. The experiments demonstrated that fibrillation more likely occurred when the chitosan content was highest.

## KEYWORDS

Coaxial electrospray; Encapsulation; Chitosan; Triclosan.

## INTRODUCTION

Chitosan (CS), a natural polysaccharide-based biopolymer derived from chitin deacetylation. It has diverse applications in drug delivery, tissue engineering, encapsulation, nano- and microparticle formation, plant protection thanks to its biocompatibility, biodegradability, low toxicity, and antibacterial properties [1–4]. Triclosan (Irgasan), another widely used antibacterial agent, is often applied on synthetic fibers like polyester, polypropylene, nylon, cellulose acetate, and acrylic, and is valued for its durability during washing [5] [6]. It can be applied on textile material by several application methods, exhaustion during or after dyeing, pad-dry-cure and melt mixing [7]. Electrospraying is increasingly recognized as an advanced method for encapsulating sensitive bioactives with minimal damage or structural loss [1] [8]. Coaxial electrospraying is also a one-stage process given in multiple studies to capsule varied materials [9–11]. Nano- and microparticles provide larger surface area and consequently allows greater bioavailability of the encapsulated substances. Several studies reported that both solution parameters as well as process parameters directly affect particle size and formation [1].

Because of chitosan's cost-effectiveness, non-toxicity, antibacterial properties, and compatibility

with biological systems, it is viewed as an ideal encapsulating agent for textile applications [12]. Several methods can be used for the formation of chitosan micro- and nanospheres, including solvent evaporation, coacervation/precipitation, ionic gelation and spray drying [13]. For microencapsulation process, techniques such as emulsification, spray drying, coaxial electrospray systems, freeze-drying, coacervation, in situ polymerization, extrusion, fluidized-bed coating, and supercritical fluid technology can be utilized [12]. Cotton fabric was treated with antimicrobial peptides encapsulated in alginate-chitosan microcapsules, for potential textile applications [14]. *O. sanctum* leaf extract was encapsulated in chitosan and applied to cotton garments, showed exceptional antibacterial activity and wash durability [15]. Hui et al. [16] microencapsulated Traditional Chinese Herbs in chitosan–sodium alginate blend matrix and grafted onto the cotton fabric's surface for the clinical treatment of atopic dermatitis. Another study reported excellent antimicrobial efficacy of electrosprayed chitosan onto wool surface [17].

Triclosan loaded chitosan and alginate-based microcapsules have been used for coating applications in surfaces such as textiles or plastics [18]. Santos Alves de Lima [5] investigated these microcapsules using 2.5 wt% to 3 wt% of triclosan in both shell and core structures produced through

\* Corresponding author: Dasdemir M., e-mail: [sgserdar@gantep.edu.tr](mailto:sgserdar@gantep.edu.tr)

emulsification method. These microcapsules were aimed for future applications in antibacterial textiles and other materials such as medical device materials and plastics [18–21]. For antibacterial purposes, triclosan, silver and chitosan were used via pad-dry-cure method and showed significant performance against Gram-positive and Gram-negative bacteria [22]. Ouerghemmi et al. [23] focused on the manufacture of core-sheath nanofibers (NFs) based on chitosan (CHT) as sheath and cyclodextrin polymer (PCD)/triclosan as core triclosan using coaxial electrospinning method. They investigated the nanofibrous structure. This study, differing from previous researches, aims to produce monodisperse distributed nanocapsules with a triclosan/chitosan core/shell structure using the coaxial electro-spray method. The influences of flow rate, core/shell flow rate ratio, and needle size on the coaxial electro-spray process, which facilitates single-step production, were systematically investigated. The resulting nanocapsule structures were characterized through SEM images, TEM images and size measurements.

## EXPERIMENTAL

### Materials

Chitosan polymer was purchased from Sigma Aldrich (448869, low molecular weight; DDA  $\leq$ 75.0%). Acetic acid (Merck & Co., Inc.) was used as solvent for chitosan. Chitosan solutions were prepared according to weight/volume percent (wt/v%) which was the ratio of solute quantity as volume in 100 unit of solution. Chitosan solutions were prepared by dissolving chitosan polymer (2 wt/v%) in acetic acid, 90/10 v/v% acetic acid/distilled water. Triclosan was purchased from Sigma Aldrich (72779,  $\geq$ 97.0%). Ethanol (Merck & Co., Inc.) was used as solvent for triclosan. Triclosan solutions were prepared by (1 wt/v%) in 50/50 v/v% ethanol/distilled water.

### Methods

The coaxial electro-spraying process was carried out using a vertically arranged electro-spraying setup which consists of a high voltage power supply (Gamma High Voltage Series ES100P), a syringe pump (New Era NE-1000X), a nozzle, and a grounded collector. Chitosan solution is fed from the outer needle tip while the triclosan solution is fed from inner needle tip through dual syringe pumps via micro pumps. The resulting samples were collected on aluminum foil (200x200 mm) placed over the grounded plate. The coaxial electro-spraying application is carried out at 2.5 kV.cm<sup>-1</sup> electrical field, 8 cm distance between the needle and collector for 5 min. Different co-fluids flow rates are studied throughout the study. First, total flow rates are arranged as 5  $\mu$ l.min<sup>-1</sup>, 10  $\mu$ l.min<sup>-1</sup>, 20  $\mu$ l.min<sup>-1</sup>, and 40  $\mu$ l.min<sup>-1</sup>. Different coaxial needle sizes were also investigated. Moreover, varied core/shell flow rates

are studied as 25/75%, 50/50% and 75/25% for 10  $\mu$ l.min<sup>-1</sup> total flow rate.

Co-axial electro-sprayed nanocapsules were examined with SEM (JEOL JSM 6390) for determining morphology. Before SEM investigation, samples were coated with Au/Pd in SC 7620 Sputter Coater. SEM pictures were taken at 5-20 kV accelerating voltage and 12-15 mm working distance with magnifications between 100 and 5000. MALVERN Zetasizer Nano ZS was also used to determine the dimension of nanocapsules. Transmission electron microscopy (TEM, FEI Tecnai G2 F30) was used to reach a high-level resolution for identification of nanocapsules' formation. Electro-sprayed nanocapsules were collected onto Cu grids during co-electro-spraying.

## RESULTS AND DISCUSSION

### Effects of Total Flow Rates on Chitosan Nanocapsule Formation

To investigate the effect of total flow rate on the formation of chitosan/triclosan nanocapsules, four different total flow rates were determined; 5  $\mu$ l.min<sup>-1</sup> (2.75/2.25), 10  $\mu$ l.min<sup>-1</sup> (5.5/4.5), 20  $\mu$ l.min<sup>-1</sup> (11/9) and 40  $\mu$ l.min<sup>-1</sup> (22/18). Core/shell flow rate ratios were calculated as 55/45%. In Figure 1, it is seen clearly flow rate of the solution has a major impact on the particle formation. At higher flow rates (20  $\mu$ l.min<sup>-1</sup> and 40  $\mu$ l.min<sup>-1</sup>), the nanocapsules began to lose their spherical morphology and exhibited a tendency to aggregate. Higher flow rates lead to the formation of larger particles as the increased supply of polymer solution causes the droplets from the needle to exceed the rate of solvent evaporation, resulting in the production of these larger particles [1,24]. Particles generated at higher flow rates exhibited a tendency to agglomerate or adhere to one another, leading to the absence of distinct independent particles [9,25]. Irregular morphology may observe due to insufficient drying time. Conversely, reducing the flow rate leads to smaller droplet formation at the needle and enhances solvent evaporation, resulting in the production of smaller particles [1]. At 5  $\mu$ l.min<sup>-1</sup> total flow rate, even though the smaller particles were seen, fibrillation was also observed which may occur at low total flow rates due to the rapid drying of nanocapsules, without sufficient time to separate from each other. At 10  $\mu$ l.min<sup>-1</sup> total flow rate, no fibrillation was observed, and the particle size was smaller compared to those at higher flow rates.

In the size distribution graph, all flow rate conditions, with the exception of 10  $\mu$ l.min<sup>-1</sup>, exhibit a measurable percentage of larger particles within the distribution. At a flow rate of 10  $\mu$ l.min<sup>-1</sup>, monodisperse distribution is observed (Figure 1). Both the SEM analysis and the particle size distributions indicated that the 10  $\mu$ l.min<sup>-1</sup> flow rate was optimal.

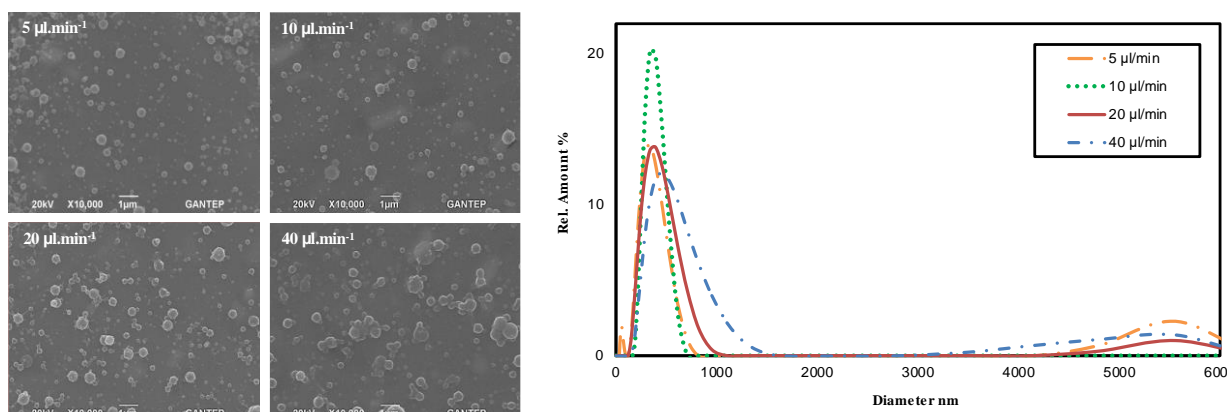


Figure 1. SEM images and size distributions (intensity) of nanocapsules at various total flow rates.

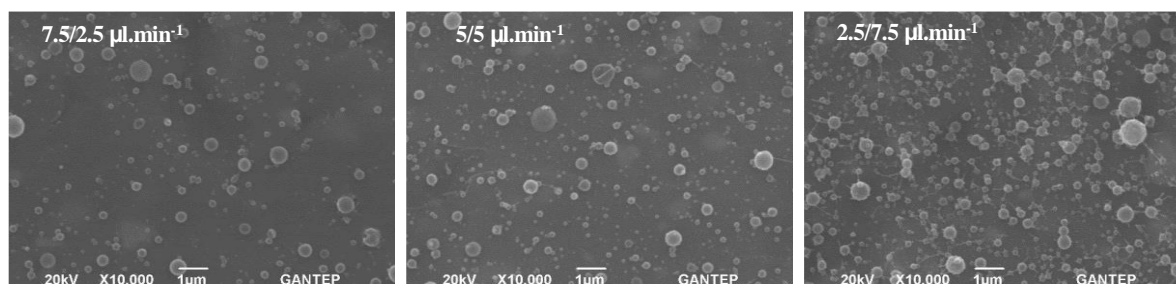


Figure 2. SEM images of nanocapsules at various core/shell flow rate ratios.

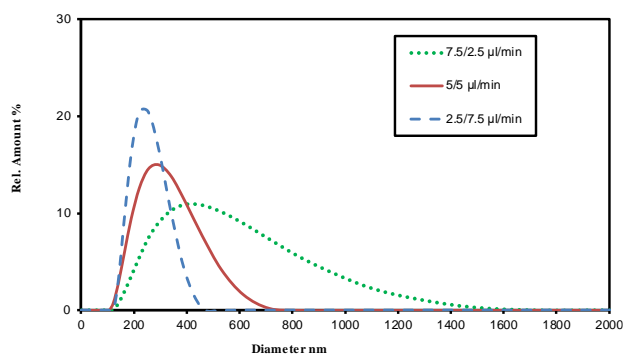


Figure 3. Size distributions (intensity) of nanocapsules at various core/shell flow rate ratios.

### Effects of Core/Shell Flow Rate Ratios on Chitosan Nanosphere Formation

A specific flow ratio between the core and shell solutions must be maintained to achieve a stable cone-jet mode during electrospaying [26]. To investigate the effects of core/shell flow rate ratios on nanocapsule formation, three different ratios were selected; 75/25%, 50/50%, 25/75%, respectively. Total flow rate was kept constant at  $10 \mu\text{l}\cdot\text{min}^{-1}$ . SEM images and size distributions of electrospayed nanocapsules at various core/shell flow rate ratios are presented in Figure 2 and Figure 3, respectively. Since the core solution, triclosan, is water-based and has a low concentration, a higher core flow rate promoted film formation. Conversely, reducing the core flow rate while increasing the shell flow rate—and thus the chitosan concentration—enhanced nanocapsule formation. As concentration rises,

interactions between chains lead to intermolecular entanglement, which limits the mobility of individual chains [27]. The lowest shell flow rate resulted in fewer particles being formed, as a low shell flow rate may lead to inadequate encapsulation of the core [28]. As the shell flow rate increased, particle formation correspondingly increased. However, at higher shell flow rate ratios, particles tended to agglomerate and fibrillate. Higher flow rates hindered complete solvent evaporation, leading to adhesion and clumping, which reduced the formation of individual particles [25].

Even though the sizes of the nanocapsules were similar at different ratios, higher chitosan content led to fibril formation between the nanocapsules. Although the  $2.5/7.5 \mu\text{l}\cdot\text{min}^{-1}$  core/shell flow rate ratio yielded the most uniform size distribution (Figure 3), because of the fibrillation, the  $5/5 \mu\text{l}\cdot\text{min}^{-1}$  core/shell flow rate ratio represented the most optimal configuration. Wang et al. [29] was reported smaller particle sizes at higher shell flow rate too.

### Effects of Needle Size on Chitosan Nanosphere Formation

Modifying the needle characteristics in electrospay processing directly affects the operating conditions and the outcomes of the process [30]. Different needles with varied gauge were employed to assess the impact of needle size on nanocapsule formation and size. Nanocapsule formation was examined using 26/22 gauge, 26/21 gauge, and 24/21 gauge needles for core/shell solutions, respectively. SEM

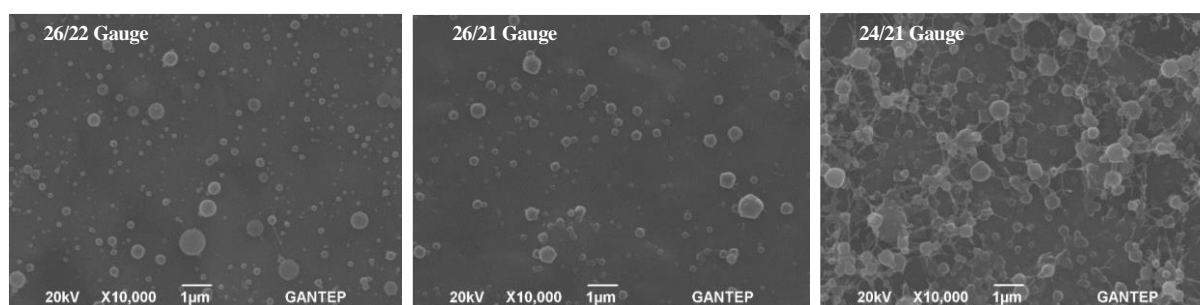


Figure 4. SEM images of nanocapsules at various needle size.

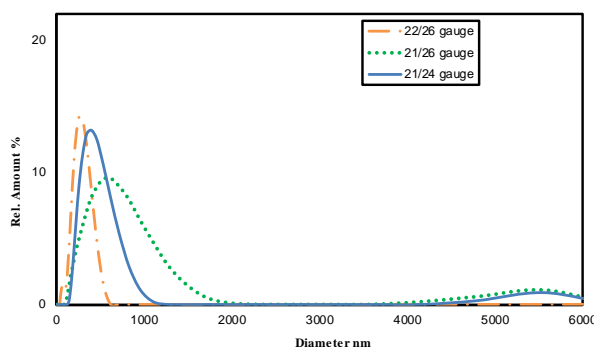


Figure 5. Size distributions of nanocapsules at various needle size (intensity).

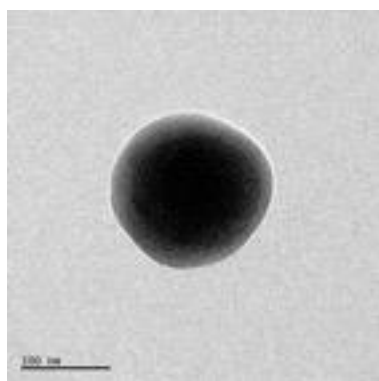


Figure 6. TEM image of nanocapsules at 5/5  $\mu\text{l}.\text{min}^{-1}$  flow rate ratio and 26/22 G needle.

images of nanocapsules produced with different needles are presented in Figure 4. Nanocapsules were successfully formed with all needle configurations. However, significant fibrillation was observed with 24/21 gauge needles. Larger needle diameter leads unseparated particles. A smaller needle diameter results in reduced droplet size at the nozzle tip due to a smaller meniscus and increased surface tension. This requires a greater Coulombic force to initiate the jet, which slows down jet acceleration and extends flight time, providing more opportunity for Rayleigh disintegration and further breakdown into smaller droplets [9]. The use of 26-gauge needle for the core solution yielded more uniform spherical structures.

The size distribution of the nanocapsules is illustrated in Figure 5. Among the configurations with comparable SEM image appearances, the 26/22 gauge needle combination demonstrated a more monodisperse distribution than 26/21 gauge.

Consequently, the 26/22 gauge needle configuration was selected to achieve better distribution.

The TEM image of the nanocapsule at a 5/5  $\mu\text{l}.\text{min}^{-1}$  flow rate ratio and a 26/22 G needle, shown in Figure 6, clearly displays both the core and the shell in spherical structure, indicating successful encapsulation.

## CONCLUSIONS

The objective of this study is to produce chitosan-based nanocapsules with a spherical structure and monodisperse distribution. To achieve this, experiments were conducted with various process parameters, including total flow rates, flow rate ratios for core/shell solutions, and core/shell needle sizes. When the total flow rate was reduced, fibrillation was observed between the capsules, while at higher rates, the capsules tended to aggregate, leading to deformation of their shapes. In the experiments focused on core/shell flow rate ratios, fibrillation was noted when the chitosan content as shell material was at its highest. In comparison with other flow rate ratios, the study with an equal core/shell ratio demonstrated the most promising size distribution. Smaller needle diameters produced smaller particles, while larger needles resulted in poorly separated capsules. The optimal results were achieved using the smallest needle gauge.

**Acknowledgement:** The authors are grateful to The Scientific and Technological Research Council of Turkey (TÜBİTAK) for funding this work (Project No: MAG-113M517).

## REFERENCES

1. Kurakula M., Raghavendra Naveen N.: Electro spraying: A facile technology unfolding the chitosan based drug delivery and biomedical applications. *Eur Polym J.*, 147, 2021, 110326 p. <https://doi.org/10.1016/j.eurpolymj.2021.110326>
2. Massella D., Giraud S., Guan J., et al.: Textiles for health: a review of textile fabrics treated with chitosan microcapsules. *Environ Chem Lett.*, 17(4), 2019, pp. 1787–1800. <https://doi.org/10.1007/s10311-019-00913-w>
3. Muñoz-Bonilla A., Echeverria C., Sonseca Á., et al.: Bio-Based Polymers with Antimicrobial Properties towards Sustainable Development. *Materials*, 12(4), 2019, 641p. <https://doi.org/10.3390/ma12040641>
4. İbili H., Dasdemir M.: Formation, Characterization and Multifunctional Activity of Chitosan Nanoparticle Coating. *Fibers Polym.*, 23, 2022, pp. 1856–1869. <https://doi.org/10.1007/s12221-022-4116-1>

5. Lima C.S.A.D., Varca G.H.C., Costa S.M.D., et al.: Development of natural polymeric microcapsules for antimicrobial drug delivery: triclosan loaded chitosan and alginate-based microcapsules. *Drug Dev Ind Pharm*, 46(9), 2020, pp. 1477–1486.  
<https://doi.org/10.1080/03639045.2020.1809445>
6. Tania I.S., Ali M., Arafat M.T.: Processing techniques of antimicrobial textiles. In: *Antimicrobial Textiles from Natural Resources*, 2021, pp. 189–215.  
<https://doi.org/10.1016/B978-0-12-821485-5.00002-0>
7. Liyanage S., Parajuli P., Hossain M.T., et al.: Antimicrobials for protective clothing. In: *Antimicrobial Textiles from Natural Resources*, 2021, pp. 349 – 376.  
<https://doi.org/10.1016/B978-0-08-100576-7.00016-X>
8. Wang J., Jansen J.A., Yang F.: Electrospinning: Possibilities and Challenges of Engineering Carriers for Biomedical Applications—A Mini Review. *Front Chem.*, 25(7), 2019, 258 p.  
<https://doi.org/10.3389/fchem.2019.00258>
9. Alfatama M., Shahzad Y., Choukaife H.: Recent advances of electrospinning technique for multiparticulate preparation: Drug delivery applications. *Adv Colloid Interface Sci.*, 325, 2024, 103098 p.  
<https://doi.org/10.1016/j.cis.2024.103098>
10. Park J.E., Kim Y.K., Kim S.Y., et al.: Biocompatibility and Antibacterial Effect of Ginger Fraction Loaded PLGA Microspheres Fabricated by Coaxial Electrospinning. *Materials*, 16(5), 2023, 1885 p.  
<https://doi.org/10.3390/ma16051885>
11. Zhang Y., Tremblay P.L., Zhang T.: Electrospun trilayer poly (d,l-lactide-co-glycolide) nanoparticles for the controlled co-delivery of a SGLT2 inhibitor and a thiazide-like diuretic. *J Drug Deliv Sci Technol*, 81, 2023, 104311 p.  
<https://doi.org/10.1016/j.jddst.2023.104311>
12. Valle J.A.B., Valle R.D.C.S.C., Bierhalz A.C.K., et al.: Chitosan microcapsules: Methods of the production and use in the textile finishing. *J Appl Polym Sci.*, 138(21), 2021, 50482 p.  
<https://doi.org/10.1002/app.50482>
13. Arya N., Chakraborty S., Dube N., et al.: Electrospinning: A facile technique for synthesis of chitosan-based micro/nanospheres for drug delivery applications. *J Biomed Mater Res B Appl Biomater*, 88B(1), 2009, pp. 17–31.  
<https://doi.org/10.1002/jbm.b.31085>
14. Antunes L., Faustino G., Mouro C., et al.: Bioactive microsphere-based coating for biomedical-textiles with encapsulated antimicrobial peptides (AMPs). *Ciênc Tecnol Mater*, 26(2), 2014, pp. 118–125.  
<https://doi.org/10.1016/j.ctmat.2015.03.006>
15. Rajendran R., Radhai R., Kotresh T.M., et al.: Development of antimicrobial cotton fabrics using herb loaded nanoparticles. *Carbohydr Polym.*, 91(2), 2013, pp. 613–617.  
<https://doi.org/10.1016/j.carbpol.2012.08.064>
16. Hui P.C.L., Wang W.Y., Kan C.W., et al.: Microencapsulation of Traditional Chinese Herbs—PentaHerbs extracts and potential application in healthcare textiles. *Colloids Surf B Biointerfaces*, 111, 2013, pp. 156–161.  
<https://doi.org/10.1016/j.colsurfb.2013.05.036>
17. Islam S., Jadhav A., Fang J., et al.: Surface Deposition of Chitosan on Wool Substrate by Electrospinning. *Adv Mater Res.*, 331, 2011, pp. 165–170.  
<https://doi.org/10.4028/www.scientific.net/AMR.331.165>
18. Silva A.C.Q., Silvestre A.J.D., Freire C.S.R., et al.: Modification of textiles for functional applications. In: *Fundamentals of Natural Fibres and Textiles*, 2011, pp. 303–365.  
<https://doi.org/10.1016/B978-0-12-821483-1.00010-3>
19. Abbaszad Rafi A., Mahkam M.: Preparation of magnetic pH-sensitive microcapsules with an alginate base as colon specific drug delivery systems through an entirely green route. *RSC Adv.*, 5(6), 2015, pp. 4628–4638.  
<https://doi.org/10.1039/C4RA15170D>
20. Elisseeff J.: Structure starts to gel. *Nat Mater*, 7(4), 2008, pp. 271–273.  
<https://doi.org/10.1038/nmat2147>
21. Karzar Jeddi M., Mahkam M.: Magnetic nano carboxymethyl cellulose-alginate/chitosan hydrogel beads as biodegradable devices for controlled drug delivery. *Int J Biol Macromol*, 135, 2019, pp. 829–838.  
<https://doi.org/10.1016/j.ijbiomac.2019.05.210>
22. Dhiman G., Chakraborty J.N.: Antimicrobial performance of cotton finished with triclosan, silver and chitosan. *Fash Text*, 2(1), 2015, 13 p.  
<https://doi.org/10.1186/s40691-015-0040-y>
23. Ouerghemmi S., Degoutin S., Maton M., et al.: Core-Sheath Electrospun Nanofibers Based on Chitosan and Cyclodextrin Polymer for the Prolonged Release of Triclosan. *Polymers*, 14(10), 2022, 1955 p.  
<https://doi.org/10.3390/polym14101955>
24. Chang M.W., Stride E., Edirisinghe M.: Controlling the thickness of hollow polymeric microspheres prepared by electrohydrodynamic atomization. *J R Soc Interface*, 2010.  
<https://doi.org/10.1098/rsif.2010.0092.focus>
25. Liu Y., Li S., Li H., et al.: Synthesis and properties of core-shell thymol-loaded zein/shellac nanoparticles by coaxial electrospinning as edible coatings. *Mater Des.*, 212, 2021, 110214 p.  
<https://doi.org/10.1016/j.matdes.2021.110214>
26. Tsai S., Ting Y.: Synthesis of alginate/chitosan bilayer nanocarrier by CCD-RSM guided co-axial electrospinning: A novel and versatile approach. *Food Res Int.*, 116, 2019, pp. 1163–1172.  
<https://doi.org/10.1016/j.foodres.2018.11.047>
27. Dasdemir M., İbili H.: Formation and characterization of superhydrophobic and alcohol-repellent nonwovens via electrohydrodynamic atomization (electrospinning). *J Ind Text*, 47(1), 2017, pp. 125–146.  
<https://doi.org/10.1177/1528083716639061>
28. Rathore P., Schiffman J.D.: Beyond the Single-Nozzle: Coaxial Electrospinning Enables Innovative Nanofiber Chemistries, Geometries, and Applications. *ACS Appl Mater Interfaces*, 13(1), 2021, pp. 48–66.  
<https://doi.org/10.1021/acsami.0c17706>
29. Wang Y., Yu D.G., Liu Y., et al.: Progress of Electrospun Nanofibrous Carriers for Modifications to Drug Release Profiles. *J Funct Biomater*, 13(4), 2022, 289 p.  
<https://doi.org/10.3390/jfb13040289>
30. Ahmad Z., Zhang H.B., Farook U., et al.: Generation of multilayered structures for biomedical applications using a novel tri-needle coaxial device and electrohydrodynamic flow. *J R Soc Interface*, 5(27), 2008, pp. 1255–1261.  
<https://doi.org/10.1098/rsif.2008.0247>